Multibeam Operations off the Coast of Madagascar

Post-Survey Modeling of Underwater Sound

Author:
Mikhail Zykov

19 September 2013

P001190-002
Document 00432
Version 1.1

JASCO Applied Sciences
Suite 202, 32 Troop Ave.
Dartmouth, NS B3B 1Z1 Canada
Phone: +1-902-405-3336
Fax: +1-902-405-3337
www.jasco.com

Suggested citation:

Zykov, M. 2012. *Multibeam Operations off the Coast of Madagascar: Post-Survey Modeling of Underwater Sound*. JASCO Document 00432, Version 1.1. Technical report by JASCO Applied Sciences

Contents

Figures

Tables

1. Introduction

JASCO Applied Sciences (JASCO) carried out an acoustic modeling study to estimate the sound levels generated by a multibeam sonar that was operated off the coast of Madagascar in summer 2008. The period of interest is 02:45 to 16:31 (UTC+3) on 29 May 2008 when the vessel was operating a multibeam sonar during transit to the Sifaka seismic survey area and during calibrations at the survey area. The sonar system considered is the Kongsberg Simrad EM 120 multibeam echosounder (MBES) with a nominal operating frequency of 12 kHz. The transducer arrays of the sonar were hull mounted, so the depth of the transducers was equal to vessel draft of 6.7 m.

The goals of this modeling study were to:

- Determine the sound source levels and the beam pattern of the Kongsberg Simrad EM 120 multibeam sonar;
- Model the sound field from the multibeam sonar;
- Estimate the maximum range from the sound source to thresholds of root-mean-square (rms) sound pressure level (SPL) from 200 to 120 dB re 1 µPa in 10 dB increments for a single pulse;
- Estimate the maximum extent of specific rms SPLs (160, 140, and 120 dB re 1 µPa) from the sonar along the entire vessel track; and
- Estimate the variation over time of the received rms SPLs from the sonar at several fixed points as the vessel progressed along the track.

Special consideration was given to the deep channel that cuts across the shelf south of Nosy Lava Island. Outside the deep channel, the water depth at the shelf break is as shallow as 2 m, so sound is effectively blocked from entering the shelf area; whereas the deep channel allows unobstructed propagation of sound waves through the shelf break, so the sonar sound would likely propagate farther within the deep channel than in the shallower areas outside the deep channel.

2. Methods

The Sifaka survey area is located offshore of northeastern Madagascar in the Mozambique Channel. The center of the 12 × 12 km block is 40 km northwest of Nosy Lava Island and 20 km from the shelf break (see Figure 1). The multibeam echosounder was operated during transit to the Sifaka survey area and along calibration tracks within the area.

Special consideration was given to the deep channel that cuts across the shelf south of Nosy Lava Island because the sonar sound would likely propagate farther within the deep channel than in the shallower areas outside the deep channel. Three scenarios of multibeam sonar operation were modeled:

1. A single sonar pulse emitted at the Sifaka survey area at the point on the vessel track closest to the deep channel;
2. Twenty-four sonar pulses emitted from various source locations along the vessel track to estimate the limits of the area ensonified to various rms SPLs; and
3. A total of 566 pulses emitted along the vessel track and received at various fixed receiver points along the deep channel to determine the temporal variation in received rms SPLs throughout the sonar operations.

The source levels and beam pattern of the Kongsberg EM 120 multibeam sonar were predicted with transducer theory. These were input into the BELLHOP version of JASCO's Marine Operations Noise Model (MONM-BELLHOP) to model the sound propagation for each of the three scenarios.

Along with the source levels and beam pattern of the EM 120, the following environmental information was input to the propagation model. High resolution bathymetry data were supplemented with lower resolution data from the global *SRTM30+* global topography and bathymetry grid (Rodriguez et al. 2005) to cover the entire modeled region. The seafloor within the region was assumed to consist of clay sediment. The sound speed profile in the water column was derived from conductivity-temperature depth measurements conducted during the sonar operations. These measurements were also used to calculate the absorption coefficient of the seawater, about 0.9 dB/km at 12 kHz.

2.1. Modeled Scenarios

The track of the vessel was reconstructed for the period from when the vessel departed Diego Suarez port on 28 May 2008 at 09:48 (GMT+3) to the completion of the calibration operations of the multibeam sonar on 29 May at 16:30. The vessel's position log is provided in Table A-1. The vessel track was reconstructed from several information sources including navigational records from the sonar operations, the vessel log of reported positions (every 4 h), and other time logs. The vessel's track is shown in Figure 1 for 28 May through 3 Jun 2008, and the period of multibeam sonar operations is shown in yellow. The sections of the track when the sonar was engaged were determined from the logs.

2.1.1. Scenario 1: Single Pulse in the Sifaka Survey Area

The goal of this scenario was to estimate the maximum range from the MBES to thresholds of rms SPLs from 200 to 120 dB re 1 µPa, in 10 dB increments, for a single sonar pulse emitted from inside the Sifaka survey area.

To produce precautionary results, the source location (star in Figure 1) was chosen to be the closest point on the vessel track to the deep channel in the shelf south of Nosy Lava Island because the sonar sound would likely propagate farther within the deep channel than in the shallower areas outside the deep channel. For this same reason, the sonar was oriented such that the broadside direction was toward the deep channel. The water depth at the source location is about 1500 m.

2.1.2. Scenario 2: Extent of rms SPLs during MBES Operations

The goal of this scenario was to estimate the limits of the area that were potentially subjected to rms SPLs of 120, 140, and 160 dB re 1 µPa during the MBES operations.

To establish the maximum extent of the specific sound levels throughout the sonar operations, sound propagation was modeled for various source locations along the vessel track. Changes in the propagation conditions along the vessel track would be exclusively due to changes in the water depth or the orientation of the sonar, so there was no need to model all the sonar pulses along the entire length of the track. Instead, the source locations were selected to include all the extremes in water depth along the track and any changes in the vessel (and sonar) heading, including the start and end of the multibeam calibration tracks. A total of 24 source locations were modeled with the broadside of the sonar beam oriented perpendicular to the on-track direction (Figure 2, Table A-2).

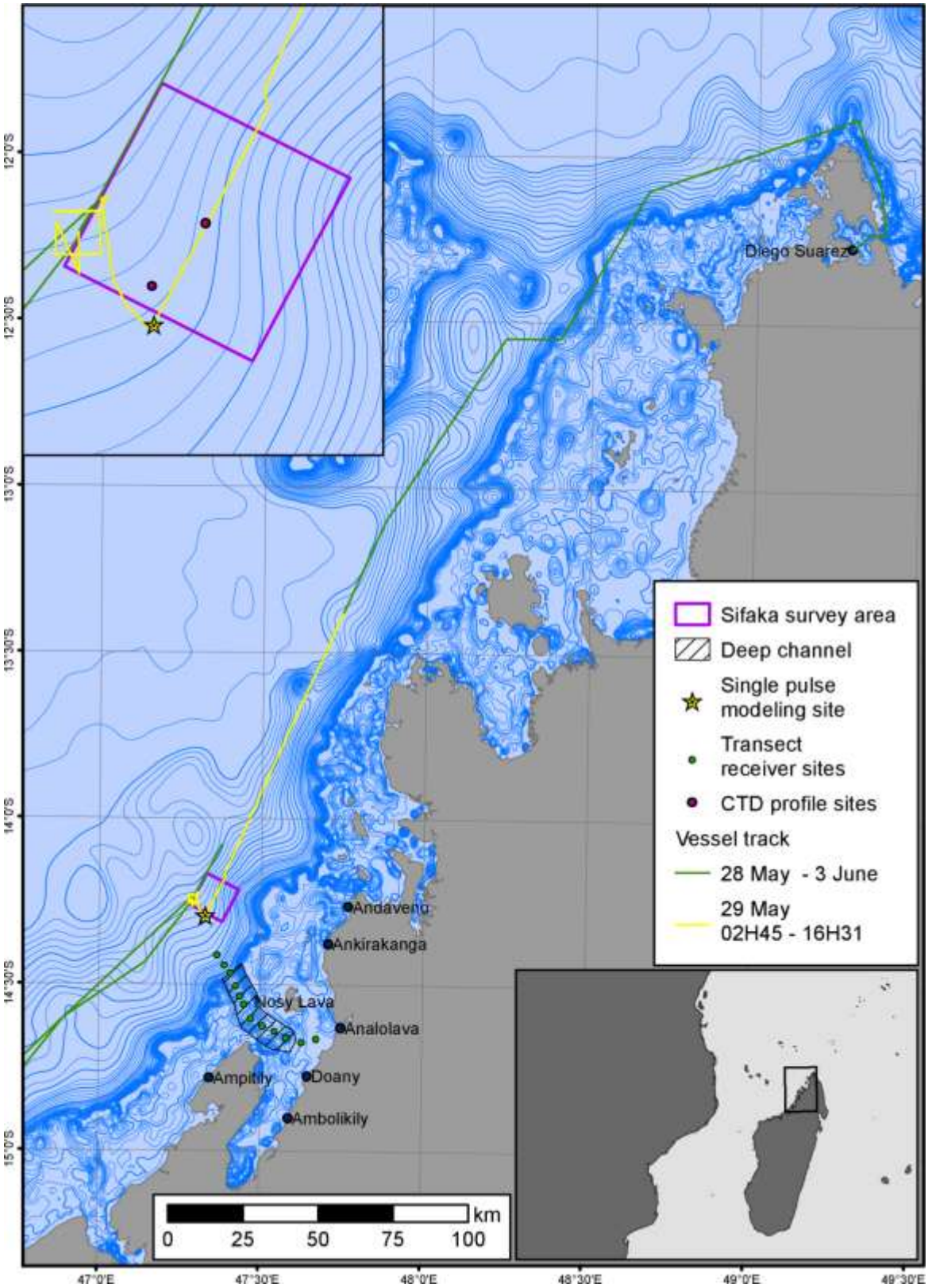

Figure 1.The Sifaka survey area in the Mozambique Channel, offshore northeastern Madagascar and the source location of Scenario 1. Times are GMT+3.

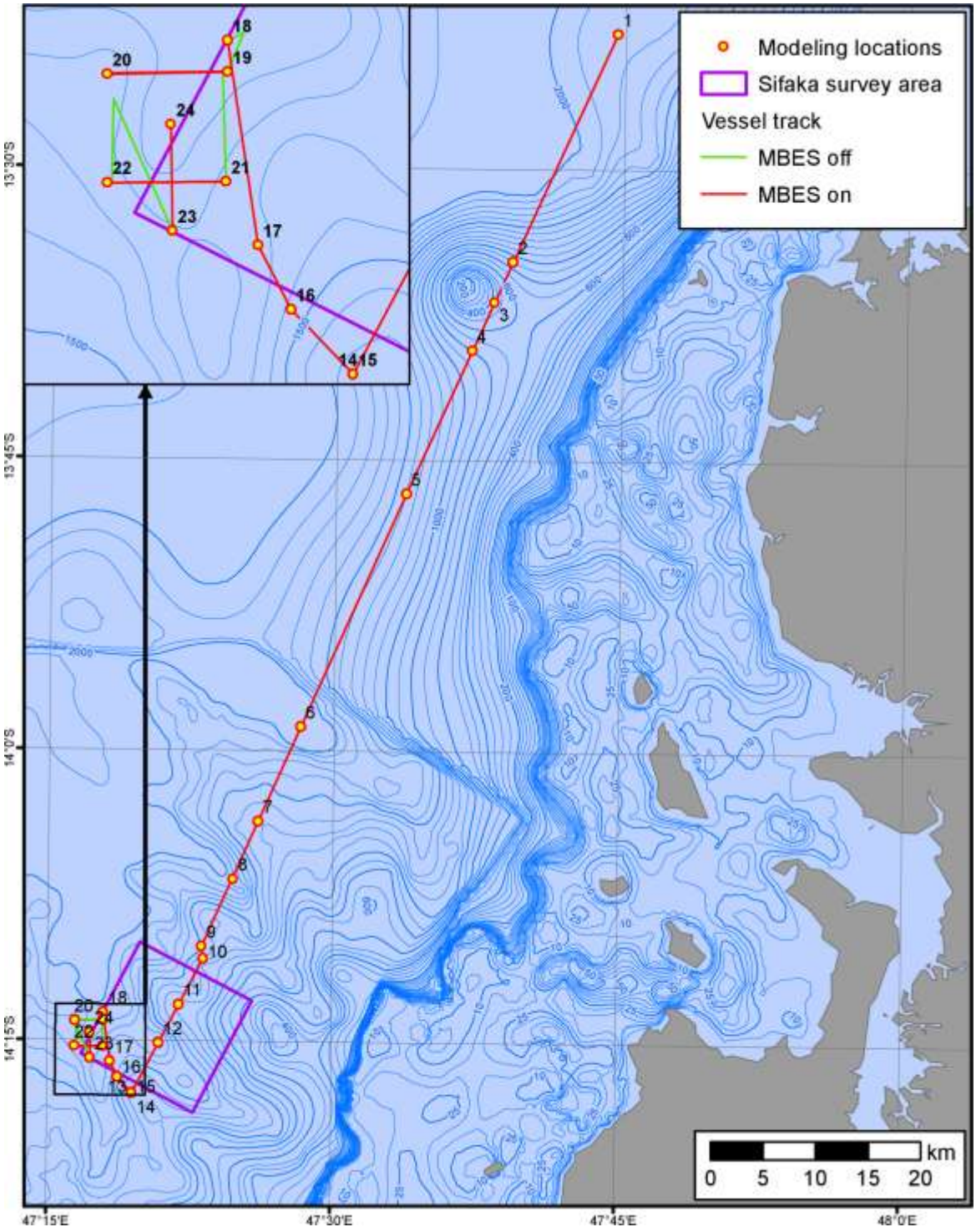

Figure 2. Scenario 2: Modeled source locations along the track that the vessel traversed from 02:45 to 16:32 (GMT+3) on 29 May 2008 at the Sifaka seismic survey area, offshore Madagascar.

2.1.3. Scenario 3: Temporal Variation in rms SPLs at Fixed Receiver Points

The goal of this scenario was to estimate the variation over time of the received maximum-over-depth rms SPLs at fixed points along a chosen transect as the vessel approached the survey area and during the multibeam calibrations. To be precautionary, the transect of receivers was placed along the deep channel in the shelf south of Nosy Lava Island because the sonar sound would likely propagate farther within the deep channel than in the shallower areas outside the deep channel. The nearest receiver point of the transect was placed on the shelf slope at 600 m water depth, and 11 more receiver points were spaced about 4 km apart along the center of the deep channel and toward the city of Analolava at water depths of 5–1000 m (Figure 3).

One sonar pulse per minute was modeled for a total of 566 source locations along the vessel track. For each source location, sound propagation was modeled within the vertical planes that connect the source location with each of the transect receiver points. The broadside beam of the sonar was oriented perpendicular to the on-track direction. The source locations were estimated from the time interval between the points (1 min) and the vessel position log (see Table A-1) assuming constant speed between the vessel waypoints. The distance between the modeled source locations along the track was 120–350 m, depending on the average transit speed between the waypoints.

Special consideration was given to Waypoint 5 of the vessel track (Figure 3), where the vessel's heading changed from 208° (east of UTM north) to 318°, i.e., a 110° turn was performed. During this turn the broadside of the sonar would have swept across the transect receiver points, exposing them to higher sound levels, so it was important to simulate this turn to account for the full exposure of the receiver points to the sonar noise. The turn was simulated by keeping the coordinates of the acoustic source constant for 5.5 min and changing only the sonar heading at a constant rate of 20° per minute. A total of 55 individual pulses were modeled, with a 0.1 min interval between pulses (i.e., 2° azimuthal step between source headings).

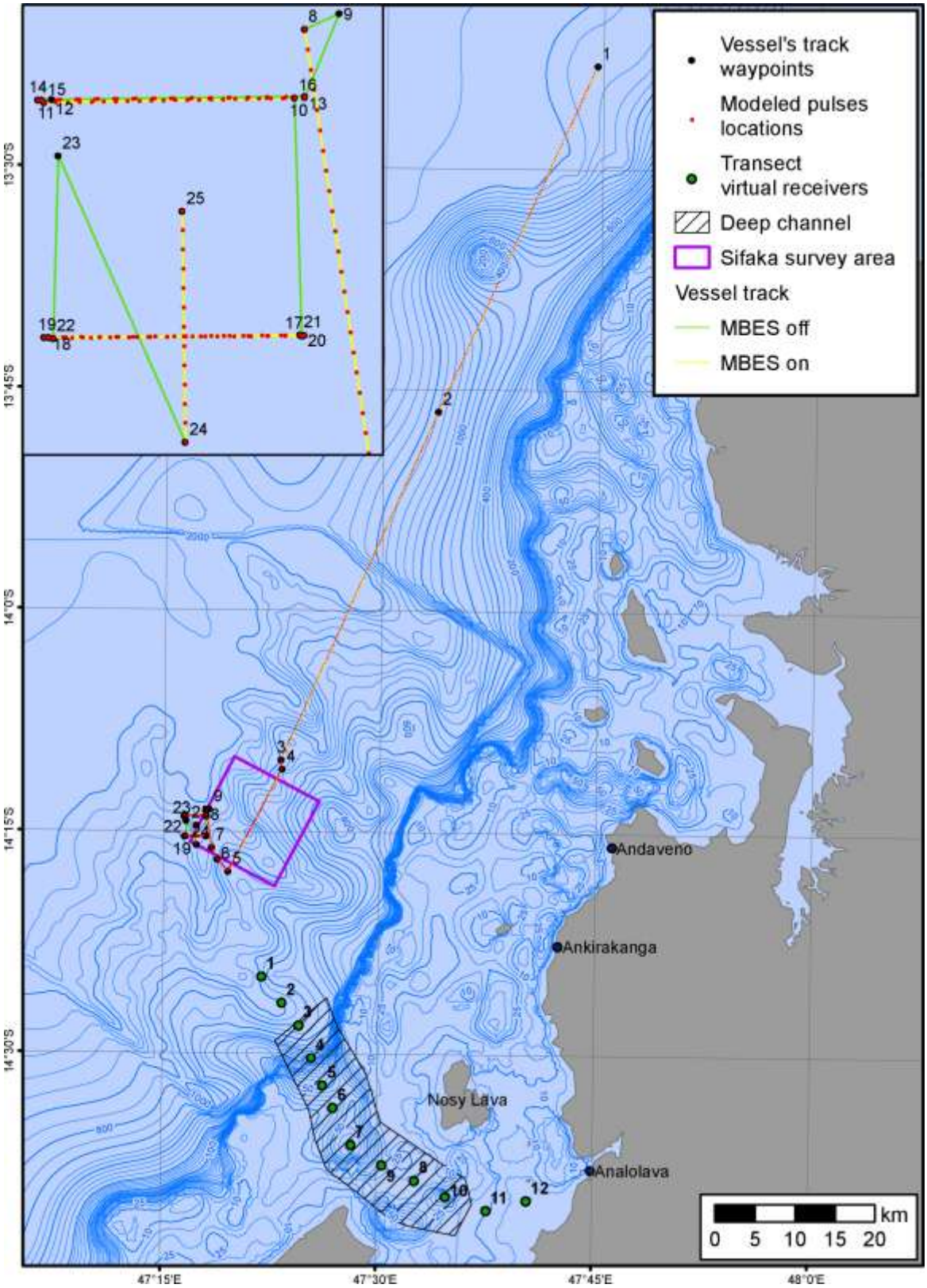

Figure 3. Scenario 3: The geometry for modeling the variation of the received root-mean-square (rms) sound pressure level (SPL) with time at fixed receiver points along a precautionary transect. The details of the vessel track waypoints are provided in Table A-1.

2.2. Acoustic Source

2.2.1. Beam Pattern Calculation

The acoustic radiation pattern, or beam pattern, of a transducer is the relative measure of acoustic transmitting or receiving power as a function of spatial angle. Directionality is generally measured in decibels relative to the maximum radiation level along the central axis perpendicular to the transducer surface. The pattern is defined largely by the operating frequency of the device and the size and shape of the transducer.

Beam patterns generally consist of a main lobe, extending along the central axis of the transducer, and multiple secondary lobes separated by nulls (example in Figure 4). The width of the main lobe depends on the size of the active surface relative to the sound wavelength in the medium, with larger transducers producing narrower beams.

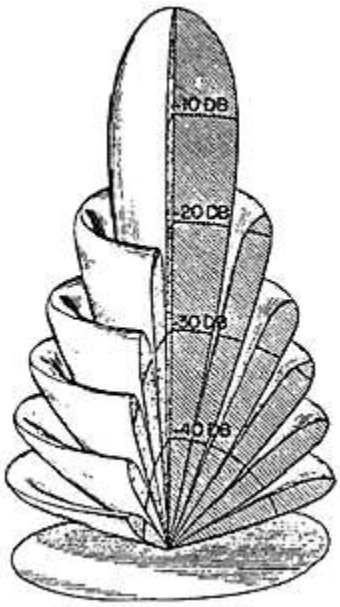

Figure 4. Typical 3-D beam pattern of a circular transducer (Massa 1999).

The beamwidth is a key characteristic of transducers. It is generally defined as the total angular range where the sound pressure level of the main beam is within 3 dB of the on-axis peak power (Massa 1999). The true beam pattern of a transducer is obtained only by *in situ* measurement of the emitted energy around the device. Such data, however, are not always available, and it is often sufficient to estimate the beam pattern based on transducer theory.

The beam directivities of a rectangular transducer can be calculated with the standard formula for the beam pattern of a rectangular acoustic array (Kinsler et al.1950, ITC 1993). This is the product of the toroidal beam patterns of two line arrays, where the directional characteristics in the along- and across-track directions are computed from the respective beamwidths. The directivity function of a toroidal beam, relative to the on-axis pressure amplitude, is:

$$R(\phi) = \frac{\sin\left(\pi\, L_\lambda \sin(\phi)\right)}{\pi\, L_\lambda \sin(\phi)} \quad , \quad L_\lambda = \frac{50}{\theta_{bw}} \tag{1}$$

where L_λ is the transducer dimension in wavelengths, θ_{bw} is the beamwidth in degrees, and ϕ is the angle from the transducer axis. Here again, the beam pattern of a transducer can be calculated using either the specified beamwidth in each plane, or the dimensions of the active surface and the operating frequency of the transducer. The calculated beam pattern for a rectangular transducer with along- and across-track beamwidths of 4° and 10°, respectively, is shown in Figure 5.

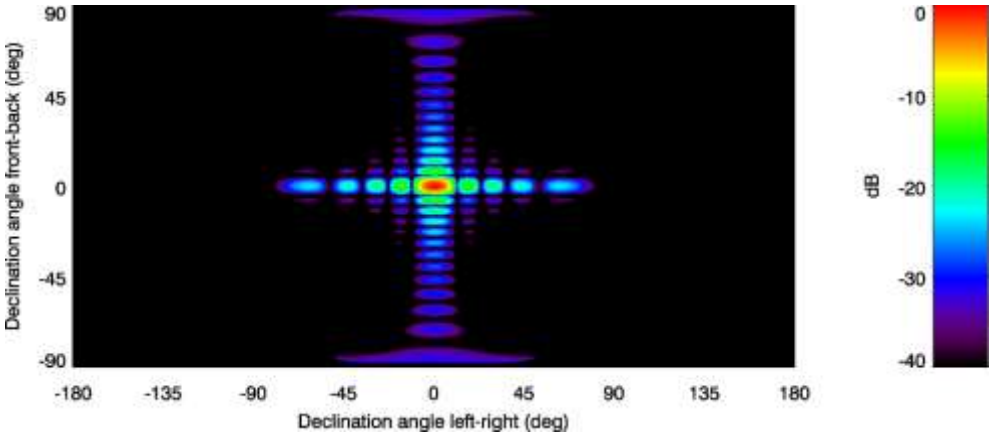

Figure 5. Calculated beam pattern for a rectangular transducer with a 4° × 10° beamwidth. Beam power function shown relative to the on-axis level, using the Robinson projection.

2.2.2. Kongsberg Simrad EM 120 Multibeam Echosounder

The Kongsberg Simrad EM 120 is a multibeam echosounder that operates at a nominal center frequency of 12 kHz for accurate sounding of the deep ocean. The transducer arrays for the sonar are hull mounted (Figure 6). The system is capable of producing 191 individual beams with a maximum angular coverage in the cross-track direction of 150°. Each individual beam has a possible width of 1° or 2°. Technical notes obtained from the manufacturer's website specify an rms SPL of 242 and 236 dB re 1 µPa @ 1 m for 1° and 2° beams, respectively (Hammerstad 2005, Kongsberg 2005). A summary of the acoustic model parameters for the Kongsberg Simrad EM 120 are presented in Table 1.

The beam patterns from the 191 simultaneously engaged beams of 2° × 2° beamwidth were calculated using Equation 1 and summed to produce the total beam pattern (150° equi-angled swath; Figure 7, Figure 8).

Figure 6. A blister for the EM 120 transmitter (Tx) and receiver (Rx) transducer arrays (2° × 2° system; ©2010 Kongsberg Maritime AS).

Table 1. Kongsberg Simrad EM 120 multibeam sonar parameters. A 2° beamwidth was assumed for all model scenarios.

	12 kHz	
Pulse duration (ms)	2, 5, or 15	
Pulse rate (Hz)	≤5	
Transducers beamwidth	1°	2°
rms SPL (dB re 1 µPa @ 1 m)	242	236
SEL per pulse (dB re 1 µPa^2·s @ 1 m)	224*	218*
Number of beams	191	
Across-track beam fan width	150°	

* Source level calculated using a pulse duration of 15 ms.

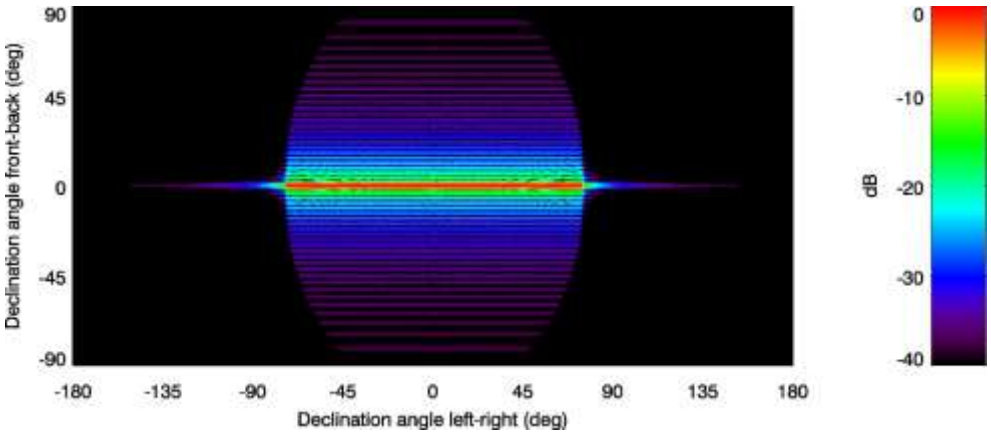

Figure 7. Calculated beam pattern for the transducer of the Kongsberg Simrad EM 120 multibeam sonar at 12 kHz. The beam power function is shown relative to the on-axis level using the Robinson projection.

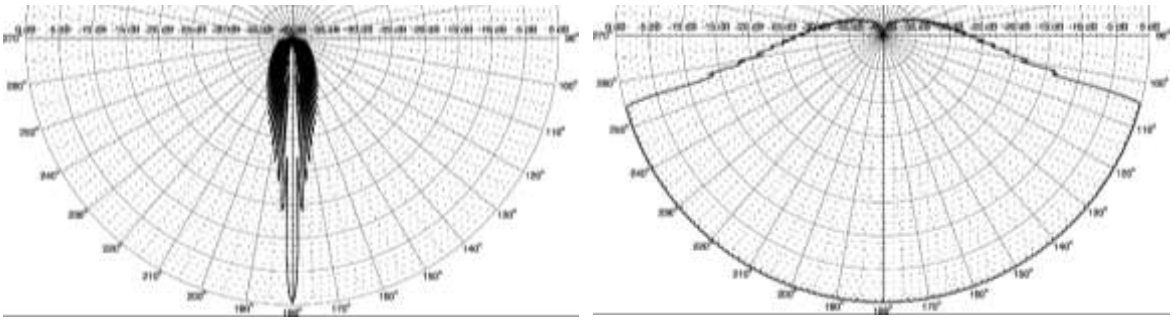

Figure 8. Calculated beam pattern vertical slice for the Kongsberg Simrad EM 120 transducer at 12 kHz in the (left) along- and (right) across-track directions.

2.3. Sound Propagation Model

2.3.1. Sound Propagation Model

Sound propagation from the EM 120 multibeam echosounder was modeled at single frequency of 12 kHz with the BELLHOP version of JASCO's Marine Operations Noise Model (MONM-BELLHOP).

MONM-BELLHOP models sound propagation in range-varying acoustic environments using the BELLHOP acoustic ray trace model (Porter and Liu 1994) that is based on the Gaussian beam tracing technique. In addition to other types of attenuation, MONM-BELLHOP accounts for sound attenuation due to energy absorption through ion relaxation and viscosity of water (Fisher and Simmons 1977). This type of attenuation is significant for frequencies higher than 5 kHz and cannot be neglected without noticeable effect on the model results at longer distances from the source.

The geoacoustic layering model for MONM-BELLHOP consists of only one interface, the sea bottom. This is an acceptable limitation because the influence of the sub-bottom layers on acoustic propagation at frequencies above 2 kHz is negligible.

The acoustic model accounts for the variability of the sound levels emitted in different directions from the source, referred to as source directivity. The source directivity is specified to the model as a function of both azimuthal and depression angle, where azimuth is the horizontal direction relative to north and depression is the vertical angle relative to the horizontal plane.

2.3.2. N×2-D Volume Approximation

MONM-BELLHOP computes acoustic fields in three dimensions by modeling transmission loss within two-dimensional (2-D) vertical planes aligned along radials covering a 360° swath from the source, an approach commonly referred to as *N*×2-D. These vertical radial planes are separated by a variable angular step size. The transmission loss is then modeled within each of the *N* vertical planes as a function of depth and range from the source.

The angular step between the modeled planes varied with azimuth relative to the across-track (broadside) direction. More planes were modeled in the near-broadside sectors (Table 2).

Table 2. Angular step size between the modeled vertical radial planes for various the various sectors azimuth.

Azimuthal angle relative to broadside	Angular step size
0–10°	0.2°
10–45°	0.5°
45–90°	1.0°

2.3.3. Sampling of Model Results: Maximum-Over-Depth Sound Levels

The received rms SPL sound field within each vertical radial plane is sampled at various ranges from the source, generally with a fixed radial step size. At each sampling range along the surface, the sound field is sampled at various depths, with the step size between samples increasing with depth below the surface. The received rms SPL at a surface sampling location is taken as the maximum value that occurs over all samples within the water column below, i.e., the *maximum-over-depth* received rms SPL. This provides a precautionary prediction of the received sound level around the source, independent of depth. These maximum-over-depth rms SPLs are presented as color contours around the source.

The vertical spacing between samples is chosen based on the vertical variability of the acoustic field. This vertical variability depends on the variability of the sound speed profile, which is higher at the top of the water column and lower at greater depths. For areas with deep water, sampling is not performed at depths beyond those reachable by marine mammal species expected in the area of interest. At each surface sampling location, the modeled sound field was sampled at the following depths before applying the maximum-over-depth rule just described:

- At 1, 4, and 7 m,
- Every 10 m from 10 to 50 m,
- Every 25 m from 75 to 200 m, and
- Every 100 m from 300 to 2000 m.

2.4. Environmental Parameters

2.4.1. Bathymetry

Several datasets were combined to create the bathymetry grid for the sound propagation model. High-resolution data for the deep water area around the survey area extend to the shelf break (approximately to the 50 m isobath) toward the shore. For the shelf area around Nosy Lava Island, isobaths and individual sounding points were digitized from a navigational (NGA chart 61420; DMA 1996). Bathymetry for the gaps between these two datasets were obtained from the *SRTM30+* (v6.0), a global topography and bathymetry grid with a resolution of 30 arc-seconds or about 1 km (Rodriguez et al. 2005). At the studied latitude, the grid cell size is about 900 × 900 m.

The *SRTM30+* bathymetry are inaccurate for the deeper parts of the area of interest due to the poor resolution. For example, the discrepancy between the high resolution bathymetry and the *SRTM30+* data is 500 m for the source location of Scenario 1 (1500 m vs. 1000 m). The

discrepancy is not expected to substantially influence the sound propagating from the multibeam sonar as the sound that is responsible for the largest contribution to the received levels travels horizontally, without sea bottom interaction. For shallower depths, the discrepancies between the high resolution bathymetry and the *SRTM30+* data are negligible.

2.4.2. Geoacoustics

A single geoacoustic profile of the seafloor was assumed for all modeled scenarios. The geoacoustic properties required by MONM-BELLHOP are as follows:

- Sediment density,
- Compression-wave (P-wave) speed, and
- P-wave attenuation coefficient (in decibels per wavelength).

These geoacoustic parameters were estimated using a sediment grain-shearing model (Buckingham 2005) by computing the acoustic properties of the sediments based on the porosity and grain size. The porosity and grain size of the sediment were selected based on the expected type of surficial sediments within the modeled region. The geoacoustic properties of the seafloor assumed for all modeled scenarios are as follows:

- Clay sediment;
- Porosity of 80%;
- Density of 1.35g/cm^3;
- P-wave speed of 1495 m/s; and
- P-wave attenuation of 0.06 dB/λ.

2.4.3. Sound Speed Profile

The sound speed in the water column was derived from two conductivity temperature depth (CTD) casts performed *in situ* during the sonar operations. The locations where the CTD profiles were measured are indicated in (Figure 1). The measured water salinity and temperature were used to calculate the sound speed in the water column down to the seabed (Figure 9). The resulting sound speed profile is strongly downward refracting. The difference between the maximum and minimum speeds is about 50 m/s. Also, there is a top layer 40 m thick that has a nearly constant sound speed of 1540 m/s.

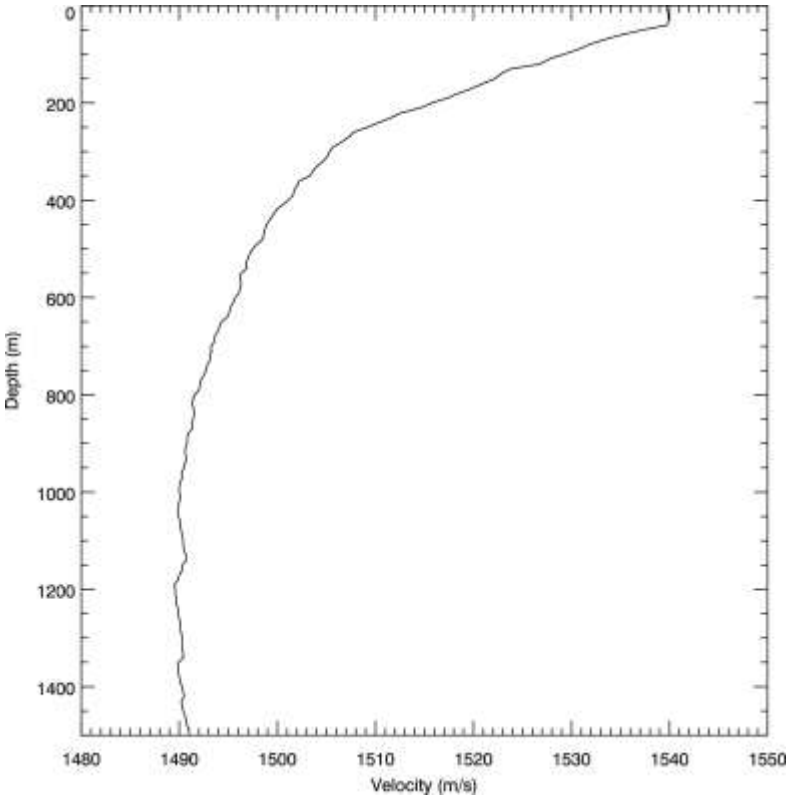

Figure 9. Sound speed profile in the water column assumed for all modeled scenarios based on two conductivity-temperature-depth (CTD) casts performed at the survey area.

2.4.4. Acoustic Energy Absorption

Propagating sound interacts with the constituents of seawater at the molecular level through a range of mechanisms, resulting in absorption of some of the sound energy (Thorp 1965, Fisher and Simmons 1977, Francois and Garrison 1982a, 1982b, Medwin 2005). This occurs even in completely particulate-free waters and is in addition to energy losses from scattering by objects such as zooplankton or suspended sediments. The absorption coefficient of the water depends on such factors as temperature, salinity, and pressure, and varies with the frequency of the acoustic wave.

The magnitude of the loss of sound energy by absorption is expressed as an attenuation coefficient in units of decibels per kilometer (dB/km). This coefficient is computed from empirical equations and generally increases with the square of the frequency. The absorption of the acoustic wave energy is virtually nil at low frequencies (below 500 Hz). It starts to have a noticeable effect (of at least 1 dB over ranges of 10–20 km) at frequencies above 1 kHz. The absorption loss increases markedly for higher frequencies: for a 100 kHz sound wave, the absorption loss can exceed 30 dB over just 1 km.

The absorption loss is an important factor for the Kongsberg EM 120 multibeam echosounder, which emits sound at 12 kHz. The estimated absorption coefficient (Figure 10) calculated using the seawater properties measured by CTD profiling is about 0.9 dB/km at 12 kHz.

MONM-BELLHOP propagation code takes the absorption effect into consideration internally.

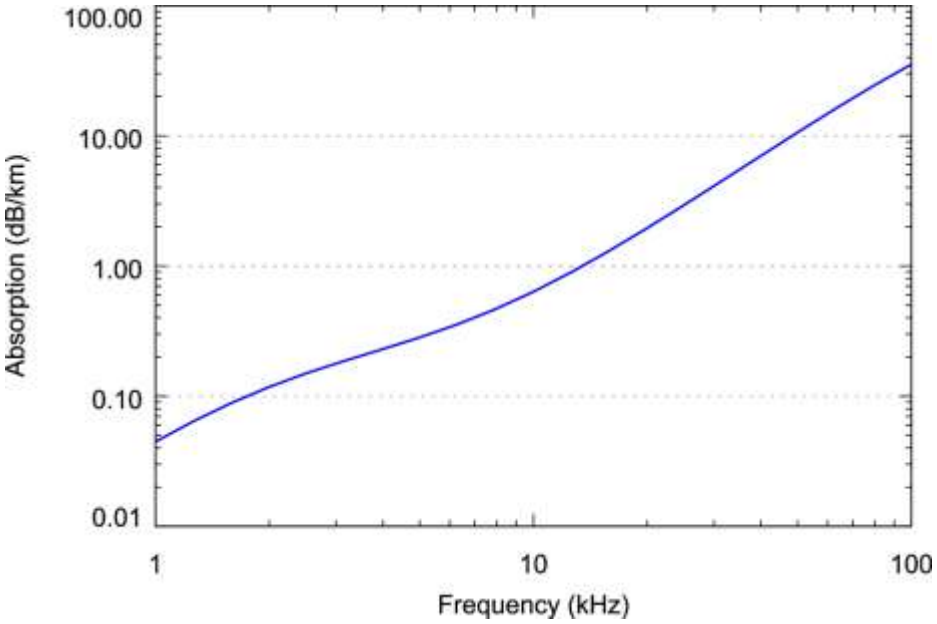

Figure 10. The acoustic energy absorption as a function of the frequency of an acoustic wave derived from CTD casts in the Mozambique Channel (27°C, 35 ppt salinity, at 40 m below sea surface).

3. Results

Sound propagation from the Kongsberg Simrad EM 120 multibeam echosounder was modeled for the operations that occurred 02:45 to 16:31 (GMT+3) on 29 May 2008 at the Sifaka survey area. The sonar was modeled at a source depth of 6.7 m. Special consideration was given to the deep channel that cuts across the shelf south of Nosy Lava Island because the sonar sound would likely propagate farther within the deep channel than in the shallower areas outside the deep channel.

A safety factor of 3 dB was added to the modeled received rms SPLs and SELs to ensure precautionary results, recognizing the inherent tendency of acoustic models to yield average expected received levels that may not fully capture real-life variability. The model results with the safety factor added provide estimates of the *maximum* expected received sound levels.

3.1. Scenario 1: Single Pulse in the Sifaka Survey Area

A single multibeam sonar pulse was modeled within the Sifaka survey area. To produce precautionary results, the source was placed at the point on the vessel track closest to the deep channel and was oriented with the broadside direction toward the deep channel (i.e., a vessel heading of 240° east of UTM north).

For each sound level threshold, two statistical estimates of the safety radius are tabulated: (1) the maximum range (R_{max}); and (2) the 95% range ($R_{95\%}$). Given a regularly gridded spatial distribution of sound levels, the $R_{95\%}$ for a given sound level is defined as the radius of the circle, centered on the source, encompassing 95% of the grid points with sound levels at or above the given value. The R_{max} for a given sound level is simply the distance to the farthest occurrence of that level (equivalent to $R_{100\%}$). R_{max} is more conservative than $R_{95\%}$ but may overestimate the effective exposure zone; for cases where the volume ensonified to a specific level is discontinuous and small pockets of higher received levels occur far beyond the main ensonified volume (e.g., due to convergence), R_{max} would be much larger than $R_{95\%}$ and could therefore be misleading if not given along with $R_{95\%}$.

Table 3 provides the maximum and 95% distances to various rms SPL thresholds. The maximum extent of the specific SEL threshold levels was also calculated (Table 4) based on the modeled rms SPL field by adjusting for the difference of the source level in SEL metrics (see Table 1). The estimated rms SPL field from a single pulse of the Kongsberg EM 120 multibeam echosounder is shown in Figure 11.

Table 3. Maximum (R_{max}, km) and 95% ($R_{95\%}$) horizontal distances from the Kongsberg EM 120 multibeam echosounder to modeled maximum-over-depth root-mean-square (rms) sound pressure level (SPL) thresholds assuming a precautionary scenario.

rms SPL (dB re 1 µPa)	R_{max} (km)	$R_{95\%}$ (km)
220	<0.02	<0.02
210	<0.02	<0.02
200	0.08	0.07
190	0.26	0.24
180	0.77	0.70
170	2.07	1.86
160	4.32	3.74
150	4.86	4.13
140	9.97	6.77
130	13.3	8.38
120	17.4	8.88

Table 4. Maximum (R_{max}, km) and 95% ($R_{95\%}$) horizontal distances from the Kongsberg EM 120 multibeam echosounder to modeled maximum-over-depth sound exposure level (SEL) thresholds assuming a precautionary scenario.

SEL (dB re 1 µPa^2·s)	R_{max} (km)	$R_{95\%}$ (km)
210	<0.02	<0.02
200	<0.02	<0.02
190	<0.02	<0.02
180	0.10	0.09
170	0.33	0.30
160	0.95	0.85
150	2.42	2.17
140	4.68	4.01
130	5.18	4.17
120	10.9	7.43

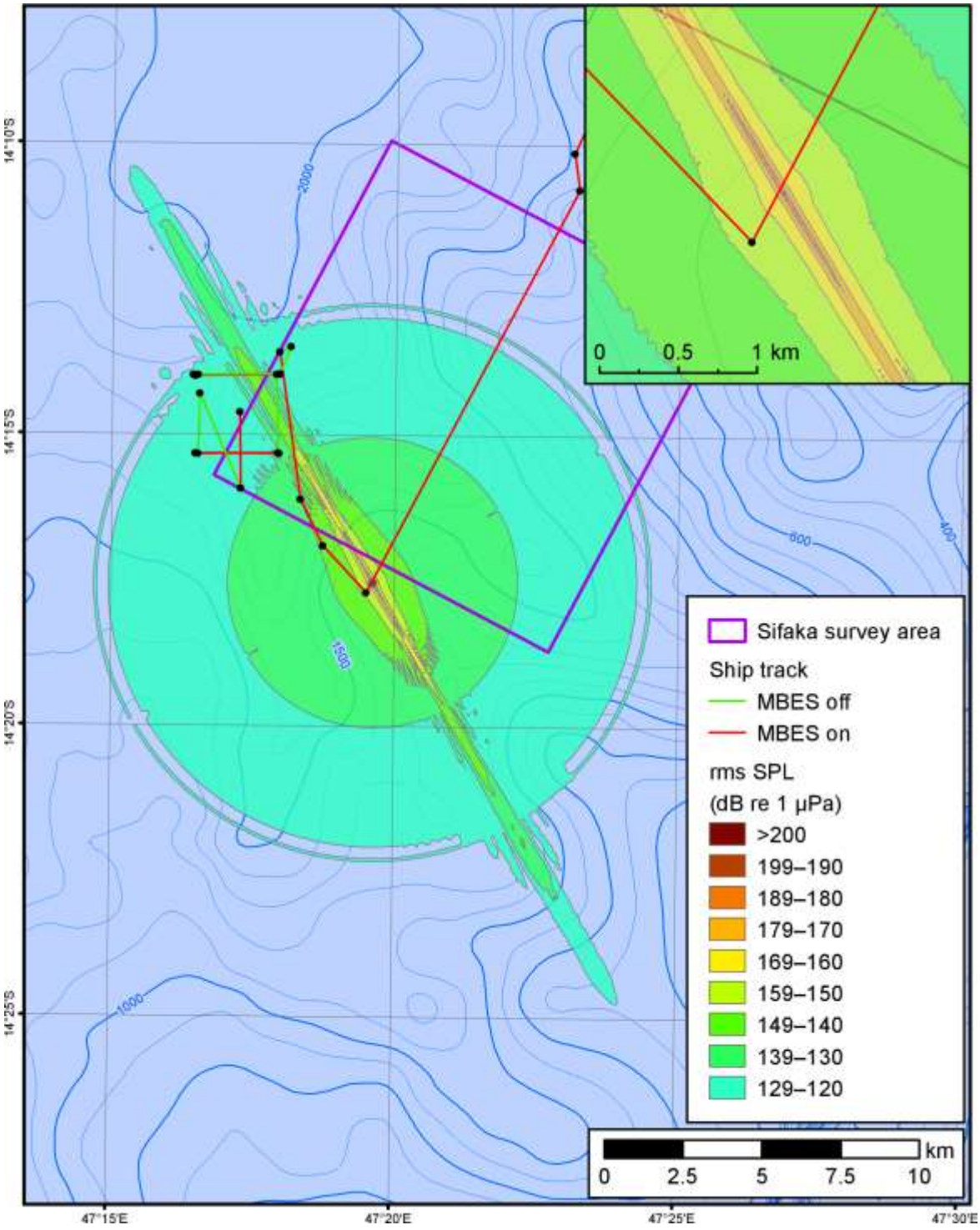

Figure 11. Modeled maximum-over-depth root-mean-square (rms) sound pressure levels (SPLs) from a single pulse from the Kongsberg EM 120 multibeam echosounder assuming a precautionary scenario.

3.2. Scenario 2: Extent of rms SPLs during the Vessel Transit

A total of 24 multibeam sonar pulses were modeled along the vessel track. The model results were processed for each source location to determine the distance to the rms SPLs thresholds of 160, 140, and 120 dB re 1 µPa (Figure 12). The envelope lines of maximum extent of the sound levels from the vessel in transit were drawn manually based on the contours resulting from the individual pulses.

Figure 13 displays the envelopes for all three threshold levels on a single map. The maximum distance to the 120 dB re 1 µPa rms SPL isopleth from the vessel track is 15.25–21.17 km, depending on the water depth and the sonar orientation (Table A-2). The maximum distance from the track to the rms SPL thresholds of 140 and 160 dB re 1 µPa is 6.95–12.52 km and 1.99–4.52 km, respectively.

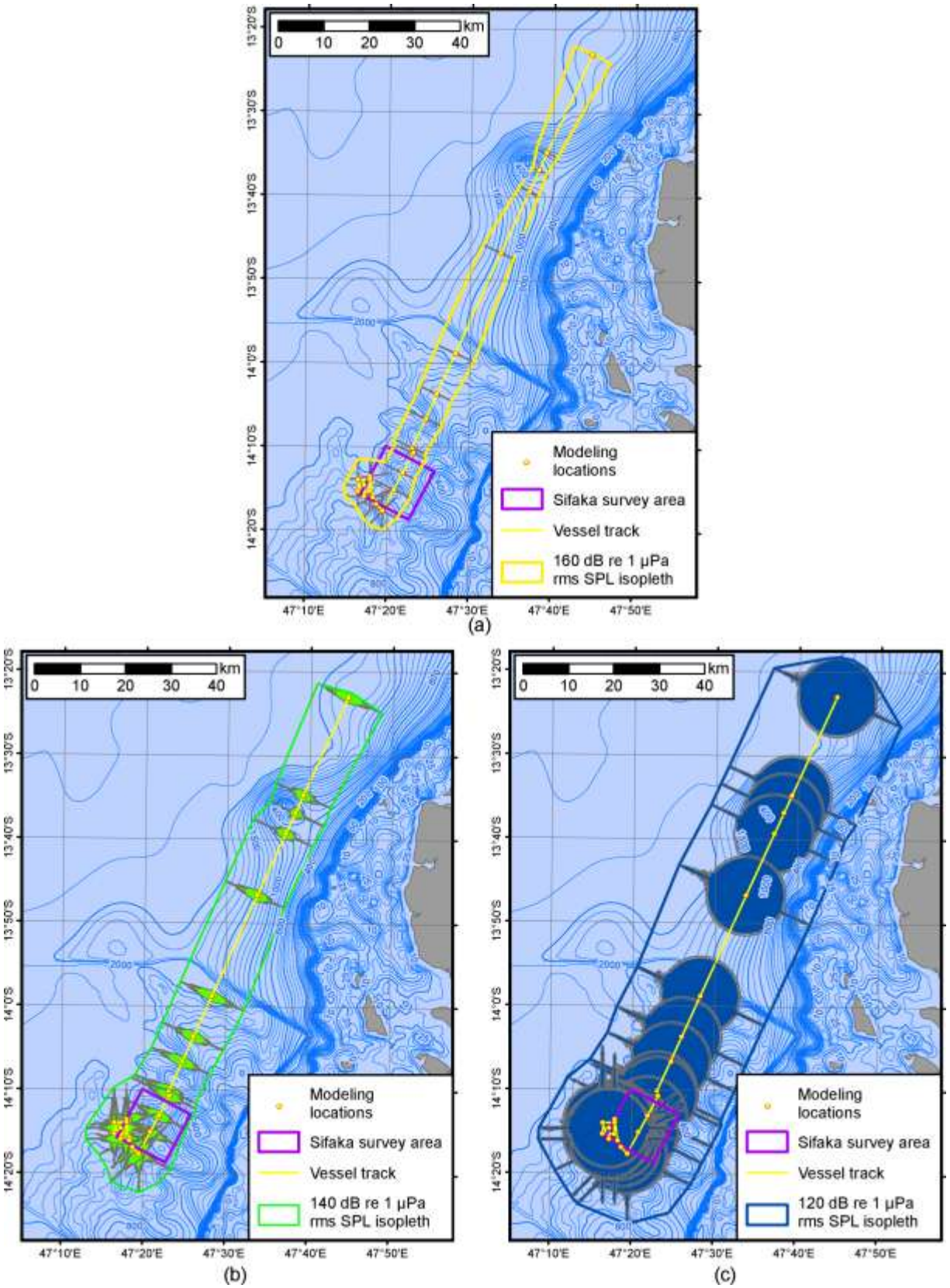

Figure 12. The (a) 120, (b) 140, and (b) 160 dB re 1 µPa maximum-over-depth root-mean-square (rms) sound pressure level (SPL) threshold contours for individual modeled pulses along the vessel track.

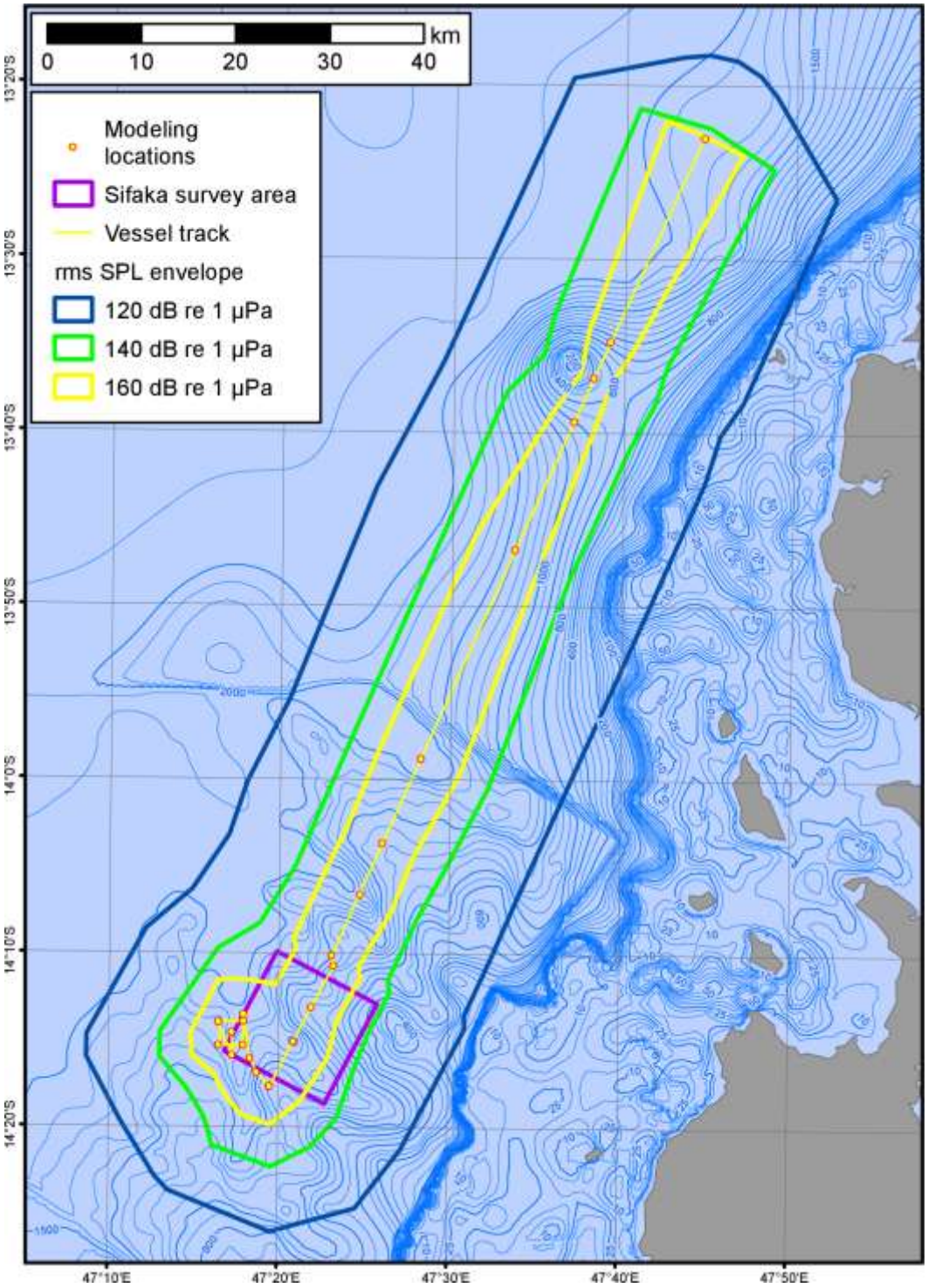

Figure 13. Maximum extension of distances to specific maximum-over-depth root-mean-square (rms) sound pressure level (SPL) thresholds around the vessel while it was operating the multibeam sonar.

3.3. Scenario 3: Temporal Variation in rms SPLs at Fixed Locations

The received rms SPLs at the selected receiver points on the precautionary transect were estimated for the multibeam sonar operations performed from 02:45 to 16:45 on 29 May 2008 (GMT+3). The maximum-over-depth rms SPL over time for each receiver point is presented in Figure 14. The model results show that no sound from the EM 120 multibeam echosounder reached receiver point 12 of the transect. The peaks in the received levels at 08:45 correspond to the vessel's turn at Waypoint 5.

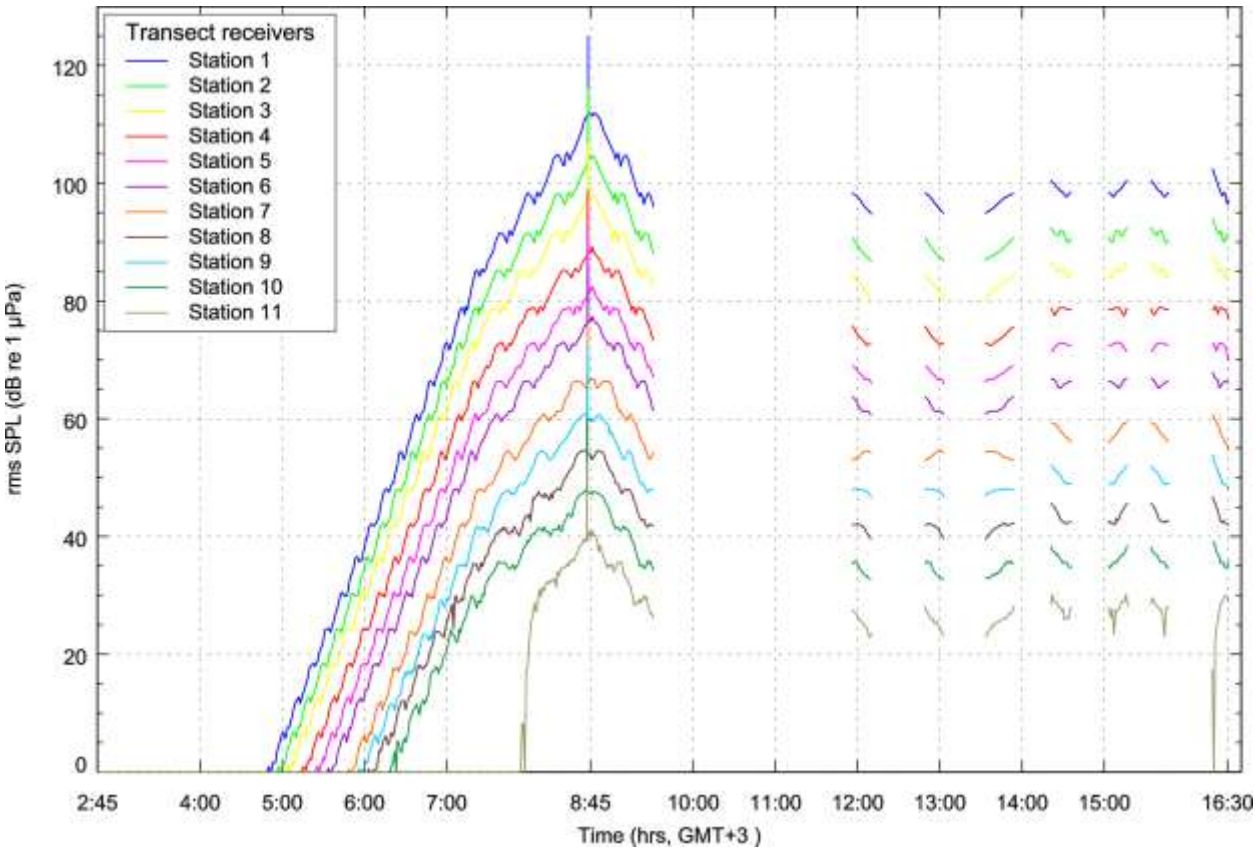

Figure 14. Received maximum-over-depth root-mean-square (rms) sound pressure level (SPL) at the virtual receivers along the precautionary transect as the vessel progressed along the track. The time period shown represents the multibeam sonar operations of 29 May 2008 (GMT+3). The gaps in the data correspond to when the sonar was off.

Literature Cited

Buckingham, M.J. 2005. Compressional and shear wave properties of marine sediments: Comparisons between theory and data. *J. Acoust. Soc. Am.* 117(1):137-152.

[DMA] Defence Mapping Agency. 1996. NGA Chart 61420. Indian Ocean. Madagascar - North Coast. Nosy-Be to Helodrano Bombetoka. 2nd Ed. February 10.

Fisher, F.H. and V.P. Simmons. 1977. Sound absorption in sea water. *J. Acoust. Soc. Am.* 62(3):558-564.

Francois, R.E. and G.R. Garrison. 1982a. Sound absorption based on ocean measurements: Part I: Pure water and magnesium sulfate contributions. *J. Acoust. Soc. Am.*. 72(3):896–907.

Francois, R.E. and G.R. Garrison. 1982b. Sound absorption based on ocean measurements. Part II: Boric acid contribution and equation for total absorption. *J. Acoust. Soc. Am.* 72:1879-1890.

Hammerstad, E. 2005. EM Technical Note: Sound Levels from Kongsberg Multibeams. September 20.

[ITC] International Transducer Corporation. 1993. *Application Equations for Underwater Sound Transducers* (pamphlet). International Transducer Corporation, Santa Barbara, CA.

Kinsler, L.E., A.R. Frey, A.B. Coppens, and J.V. Sanders. 1950. *Fundamentals of Acoustics*. John Wiley & Sons Inc., New York.

Kongsberg. 2005. *EM 120: 12 kHz multibeam echo sounder. Seabed mapping to full ocean depth* (pamphlet).

Massa, D.P. 1999. *Choosing and ultrasonic sensor for proximity or distance measurement; part 2: Optimizing sensor selection*. *Sensors*. March 1, 1999. http://www.sensorsmag.com/sensors/acoustic-ultrasound/choosing-ultrasonic-sensor-proximity-or-distance-measurement-838

Medwin, H. 2005. *Sounds in the Sea*. Cambridge University Press, Cambridge, UK.

Porter, M.B. and Y.C. Liu. 1994. Finite-element ray tracing. *Proceedings of the International Conference on Theoretical and Computational Acoustics*, Eds. D. Lee and M.H. Schultz (World Scientific, Singapore): 947-956.

Rodriguez, E., C.S. Morris, Y.J.E. Belz, E.C. Chapin, J.M. Martin, W. Daffer, and S. Hensley. 2005. *An Assessment of the SRTM Topographic Products*. JPL D-31639. Jet Propulsion Laboratory, Pasadena, CA.

Thorp, W.H. 1965. Deep-ocean sound attenuation in the sub- and low-kilocycle-per-second region. *J. Acoust. Soc. Am.* 38:648–654.

Appendix A. Vessel Positions and Modeled Source Locations

Table A-1. Vessel's known position log for the time period from 02:45 to 16:31 on 29 May 2008 (GMT+3).

Waypoint	Date	Time	MBES	Description	Latitude	Longitude	UTM Zone 38 (south)	
							X	Y
1	29May08	02:45	on		13° 23.005' S	47° 44.563' E	797063	8518816
2	29May08	05H00	on	Heading to Sifaka site survey	13° 46.500' S	47° 33.800' E	777166	8475680
3	29May08	07H25	on		14° 10.133' S	47° 23.110' E	757453	8432283
4	29May08	07H32	on		14° 10.760' S	47° 23.199' E	757600	8431126
5	29May08	08H46	on		14° 17.702' S	47° 19.501' E	750817	8418388
6	29May08	09H01	on		14° 16.900' S	47° 18.733' E	749451	8419880
7	29May08	09H09	on		14° 16.107' S	47° 18.328' E	748737	8421350
8	29May08	09H31	off		14° 13.576' S	47° 17.946' E	748096	8426025
9	29May08	10H35	off	First CTD deployment	14° 13.484' S	47° 18.145' E	748455	8426192
10	29May08	11H56	on		14° 13.964' S	47° 17.947' E	748090	8425311
11	29May08	12H10	off		14° 13.978' S	47° 16.424' E	745351	8425312
12	29May08	12H22	off	Multibeam calibration	14° 13.976' S	47° 16.503' E	745492	8425314
13	29May08	12H49	on		14° 13.958' S	47° 17.947' E	748090	8425320
14	29May08	13H03	off		14° 13.977' S	47° 16.446' E	745390	8425312
15	29May08	13H33	on		14° 13.994' S	47° 16.460' E	745415	8425282
16	29May08	13H54	off		14° 13.967' S	47° 17.889' E	747987	8425306
17	29May08	14H21	on		14° 15.322' S	47° 17.930' E	748034	8422805
18	29May08	14H36	off		14° 15.332' S	47° 16.488' E	745440	8422813
19	29May08	15H03	on		14° 15.331' S	47° 16.460' E	745391	8422815
20	29May08	15H17	off		14° 15.319' S	47° 17.943' E	748058	8422810
21	29May08	15H34	on		14° 15.317' S	47° 17.920' E	748017	8422815
22	29May08	15H47	off		14° 15.336' S	47° 16.512' E	745483	8422805
23	29May08	16H00	off		14° 14.297' S	47° 16.542' E	745556	8424721
24	29May08	16H19	on		14° 15.929' S	47° 17.267' E	746831	8421698
25	29May08	16H31	off		14° 14.612' S	47° 17.249' E	746822	8424128

Table A-2. Modeled site details and results: coordinates of the source, bearing, water depth, and the maximum distances to thresholds of root-mean-square (rms) sound pressure level (SPL) from the sonar for the modeling described in Section 2.1.2.

Source location	UTM Zone 38S		Bearing (re UTM north)	Water depth (m)	Maximum distance to rms SPL threshold (km)		
	Northing	Easting			160 dB re 1 µPa	140 dB re 1 µPa	120dB re 1 µPa
1	797092	8518779	205	1837	4.46	8.26	15.41
2	787098	8497211	205	895	2.63	6.95	15.56
3	785327	8493373	205	438	1.99	7.05	15.25
4	783208	8488779	205	798	2.41	7.80	15.35
5	776951	8475207	205	1396	4.46	8.10	18.01
6	766907	8453097	205	2260	4.46	8.08	15.43
7	762842	8444147	205	1337	4.14	11.05	16.65
8	760455	8438650	205	1900	4.44	8.66	15.41
9	757452	8432283	205	1488	4.47	8.68	19.84
10	757600	8431126	206	1370	4.47	9.45	18.16
11	755275	8426761	206	1189	4.52	11.94	21.17
12	753342	8423130	206	1834	4.47	8.27	18.30
13	750816	8418387	206	1279	4.43	11.13	17.32
14	750816	8418387	270	1279	4.36	9.22	17.88
15	750821	8418385	315	1279	4.36	12.52	18.40
16	749451	8419879	315	1572	4.47	8.68	19.94
17	748736	8421350	155	1732	4.46	8.54	16.65
18	748096	8426024	171	1959	4.42	8.10	15.41
19	748090	8425311	270	1930	4.48	8.68	17.94
20	745414	8425281	270	1761	4.46	8.22	17.42
21	748034	8422804	270	1777	4.46	8.10	15.42
22	745391	8422815	270	1753	4.44	9.56	18.94
23	746830	8421697	0	1794	4.26	8.12	15.50
24	746822	8424127	0	1967	4.48	8.26	15.42